Manipulating Nanoparticle Size within Polyelectrolyte Multilayers via Electroless Nickel Deposition

Tom C. Wang,† Michael F. Rubner,‡ and Robert E. Cohen*,†

Departments of Chemical Engineering and Materials Science and Engineering and the Center for Materials Science and Engineering, Massachusetts Institute of Technology, Cambridge, Massachusetts 02139

Received September 17, 2002. Revised Manuscript Received November 6, 2002

Palladium nanoparticles within polyelectrolyte multilayers of poly(allylamine hydrochloride) (PAH) and poly(acrylic acid) (PAA) were prepared as seeds for further growth by electroless nickel deposition. The seeds were generated by binding tetraaminepalladium from aqueous solution to PAA carboxylic acid functionalities in the polymer film and subsequent reduction. Nickel was electrolessly deposited on the small, 2-nm-diameter catalytic particles. By manipulation of the rate and duration of the electroless deposition, a nickel shell of arbitrary thickness could be grown; up to 14-nm-diameter particles were obtained. Elemental analyses showed that the composition of the electrolessly deposited material, nickel with several weight percent boron, was similar to that obtained from macroscopic surface electroless nickel plating. The electroless chemistry facilitated control over nanoparticle size independent of the process of nanoparticle nucleation and hence particle concentration.

Introduction

The chemical synthesis of hard inorganic solids directly within a soft (e.g., polymeric) matrix is an effective and facile approach for preparing nanocomposites. These materials combine the processing advantages of polymers with the electrical, optical, or magnetic properties unique to inorganics. Polyelectrolyte multilayer thin films assembled by layer-by-layer (LbL) processing are versatile matrixes for nanocomposites; LbL assembly affords nanoscale control over the internal architecture, facile and environmentally friendly processing of both simple and complex structures, and conformal and large-area coating onto a wide variety of surfaces.[1] We have demonstrated the versatility of using polyelectrolyte multilayers to selectively prepare in situ metallic and semiconductor nanoparticles via the controlled binding of metal cations and their subsequent precipitation (e.g., by reduction) within the polymeric matrix.[2] Recently, others have shown alternative syntheses of inorganic particles within pre-assembled multilayer films.[3−6] Our methodology affords facile control over the concentration, spatial distribution, and size of inorganic nanoparticles via the multilayer assembly conditions and the repeated cycling of the synthetic process.[7] In this paper we report a complementary synthetic methodology based on the electroless deposition of nickel within polyelectrolyte multilayers that facilitates manipulation of the size of previously formed nanoparticles in the multilayer.

The nanoparticle sizes and concentrations that are obtainable via in situ synthesis within polyelectrolyte multilayers and other solid polymers[8] are often limited by the availability of nanoparticle precursors due to either slow mass transfer of the precursors into the polymer or the finite concentration of precursor binding sites. Thus, the obtainable range of particle sizes is limited and, moreover, the nanoparticle concentration and size often cannot be controlled independently, with larger particles following higher concentrations. In contrast, in solution synthesis of nanoparticles, one strategy for preparing highly monodisperse nanoparticles independent of nanoparticle concentration is to separate the particle nucleation and growth events. This can be accomplished kinetically by having a much faster nucleation rate relative to the particle growth rate.[9] An alternative route to monodisperse particles is to physically separate the nucleation and growth events by using small, prenucleated nanoparticles as seeds for further growth. With a large, relatively inexhaustible source of precursor available to the seeds, nanoparticles can be grown to arbitrarily large sizes. Recently, nu-

* To whom correspondence should be addressed. E-mail: recohen@mit.edu.

† Department of Chemical Engineering and the Center for Materials Science and Engineering.

‡ Department of Materials Science and Engineering and the Center for Materials Science and Engineering.

(1) See reviews: (a) Decher, G. *Science* **1997**, *277*, 1232−1237. (b) Bertrand, P.; Jonas, A.; Laschewsky, A.; Legras, R. *Macromol. Rapid Commun.* **2000**, *21*, 319−348. (c) Hammond, P. T. *Curr. Opin. Colloid Interface Sci.* **2000**, *4*, 430−442.

(2) Joly, S.; Kane, R.; Radzilowski, L.; Wang, T.; Wu, A.; Cohen, R. E.; Thomas, E. L.; Rubner, M. F. *Langmuir* **2000**, *16*, 1354−1359.

(3) Dutta, A. K.; Ho, T.; Zhang, L.; Stroeve, P. *Chem. Mater.* **2000**, *12*, 1042−1048.

(4) Liu, J.; Cheng, L.; Song, Y.; Liu, B.; Dong, S. *Langmuir* **2001**, *17*, 6747−6750.

(5) Dai, J.; Bruening, M. L. *Nano Lett.* **2002**, *2*, 497−501.

(6) Antipov, A. A.; Sukhorukov, G. B.; Fedutik, Y. A.; Hartmann, J.; Giersig, M.; Möhwald, H. *Langmuir* **2002**, *18*, 6687−6693.

(7) Wang, T. C.; Rubner, M. F.; Cohen, R. E. *Langmuir* **2002**, *18*, 3370−3375.

(8) See reviews: (a) Beecroft, L. L.; Ober, C. K. *Chem. Mater.* **1997**, *9*, 1302−1317. (b) Cohen, R. E. *Curr. Opin. Solid State Mater. Sci.* **1999**, *4*, 587−590.

(9) Murray, C. B.; Norris, D. J.; Bawendi, M. G. *J. Am. Chem. Soc.* **1993**, *115*, 8706−8715.

10.1021/cm020934h CCC: $25.00
Published on Web 12/10/2002

Scheme 1. Schematic of the in Situ Pd Nanoparticle Synthesis and Subsequent Particle Growth by EN Deposition (Not To Scale)

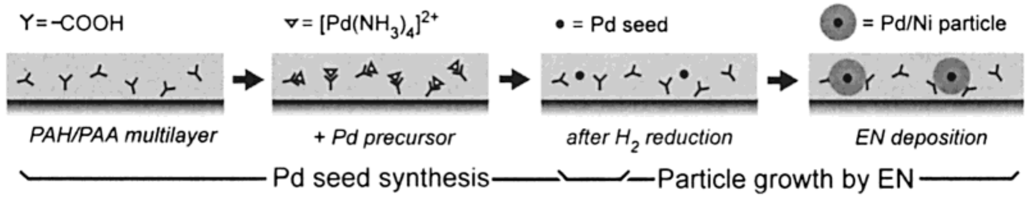

merous seeding procedures to synthesize homogeneous, single-element,[10−12] and heterogeneous[13−17] nanoparticles have been reported. For metallic nanoparticles, the selective reduction of metal precursors only on the surface of the seed particles and not in the bulk solution, which will nucleate undesirable new particles, is of primary importance in obtaining size control and monodispersity.

In our approach, we employed Pd nanoparticles synthesized within polyelectrolyte multilayers as seeds for further growth. Previous work in this area has shown nanoparticle preparation in only discrete time steps that does not offer continuous growth, and hence continuous size manipulation, of the particles. Electroless nickel (EN) chemistry[18] was used to reduce a nickel precursor selectively on the seeds. The electroless metal deposition controlled nanoparticle size independent of the initial nanoparticle seed concentration. Others have demonstrated electroless metal deposition within a polymer film containing catalytic metals but have not used this method to prepare controlled-size nanoparticles.[19−21] This methodology overcomes some limitations of our earlier cyclical binding and reaction approach by facilitating access to a virtually inexhaustible source of precursor inorganic material (i.e., the EN solution) and the continuous growth of nanoparticles without new particle nucleation.

Experimental Section

Materials. Poly(allylamine hydrochloride) (PAH) (M_w = 70 000), poly(sodium 4-styrenesulfonate) (PSS) (M_w = 70 000), tetraaminepalladium chloride ($Pd(NH_3)_4Cl_2$), and nickel sulfate hexahydrate were obtained from Sigma-Aldrich (St. Louis, MO). Poly(acrylic acid) (PAA) (M_w = 90 000) was obtained from Polysciences (Warrington, PA). Dimethylamine borane (DMAB) was obtained from Acros Organics (Fair Lawn, NJ), and sodium citrate and lactic acid were obtained from Alfa Aesar (Ward Hill, MA). All chemicals were used without further purification. Deionized water (>18 MΩ-cm, Millipore Milli-Q) was exclusively used in all aqueous solutions and rinsing procedures.

Thin Film Assembly. PAH/PAA multilayers were fabricated on glass microscope slides, polystyrene (PS) tissue−culture substrates (corona-treated, Nalge Nunc International, Naperville, IL), or polished single-crystal Si wafers using an automated Zeiss HMS slide stainer. Glass substrates and Si wafers were degreased in a detergent solution followed by air plasma treatment (5 min at 100 W, Harrick Scientific PDC-32G plasma cleaner/sterilizer) prior to deposition. PS substrates were used as received. PAH and PAA aqueous solutions (10^{-2} M by repeat unit) were adjusted to the desired pH with either 1 M HCl or 1 M NaOH. Multilayers were formed by first immersing substrates into the PAH solution for 15 min followed by three 2-min immersions into water as rinsing steps. The substrates then were immersed into the PAA solution for 15 min followed by identical rinsing steps. A single adsorption of a polycation and a polyanion is referred to as a bilayer. The adsorption and rinsing steps were repeated until the desired number of bilayers was obtained. Multilayers of PAH and PSS (10^{-2} M by repeat unit) multilayers were similarly assembled. The film was finally dried with a stream of air and stored under ambient conditions.

Preparation of Palladium Seeds. Pd nanoparticle seeds were synthesized within PAH/PAA multilayer films, as depicted in Scheme 1, using $[Pd(NH_3)_4]^{2+}$ as the precursor cationic metal complex (chloride salt). The film was immersed in an aqueous solution of the precursor (5 mM) for 30 h followed by a 1-h immersion in water as a rinsing step. After drying with a stream of air, the film containing the bound Pd complex was sealed in a H_2 atmosphere (2 atm, 85 °C) for 30 h to reduce and precipitate the Pd(II) to zerovalent Pd nanoparticles.

Nickel Deposition. The EN formulation consisted of 40 g/L nickel sulfate hexahydrate, 20 g/L sodium citrate, 10 g/L lactic acid, and 1 g/L DMAB in water.[18] A nickel stock solution of all components except the DMAB reductant was prepared in advance. A DMAB aqueous solution was prepared separately. The stock solutions were prepared for a 4:1 volumetric proportion of nickel-to-reductant stocks in the final electroless bath. They were mixed as needed and, if necessary, adjusted to a higher pH with ammonium hydroxide; the unadjusted pH of the EN solution was 3.3, measured using a pH meter (Thermo Orion model 230A+). Stock solutions were used within a week of preparation, after which they were discarded. The film containing Pd nanoparticles was immersed in the EN solution (100−200 mL) at room temperature for seeded particle growth. In certain cases, a nitrogen bubbler was employed to agitate and deoxygenate the EN solution during deposition.

Characterization. For transmission electron microscopy (TEM) imaging, multilayer films deposited on PS substrates were cut in a direction normal to the film plane using a RMC MT-X ultramicrotome with a diamond knife (Diatome, Fort Washington, PA) at room temperature. Approximately 50-nm-thick cross sections of the samples were obtained. TEM imaging was performed on ultramicrotomed samples using a JEOL JEM-2000FX operated at 200 kV. Digitized TEM images were electronically scanned from the original film negatives. Contrast enhancement was applied, if necessary; no other digital image processing was performed. Particle size distributions were obtained by measuring the diameters of at least 100 particles in high-resolution, digitized TEM images; images

(10) Brown, K. R.; Natan, M. J. *Langmuir* **1998**, *14*, 726−728.
(11) Brown, K. R.; Walter, D. G.; Natan, M. J. *Chem. Mater.* **2000**, *12*, 306−313.
(12) Jana, N. R.; Gearheart, L.; Murphy, C. J. *Chem. Mater.* **2001**, *13*, 2313−2322.
(13) Schmid, G.; Lehnert, A.; Malm, J. O.; Bovin, J. O. *Angew. Chem., Int. Ed. Engl.* **1991**, *30*, 874−876.
(14) Bright, R. M.; Walter, D. G.; Musick, M. D.; Jackson, M. A.; Allison, K. J.; Natan, M. J. *Langmuir* **1996**, *12*, 810−817.
(15) Yu, H.; Gibbons, P. C.; Kelton, K. F.; Buhro, W. E. *J. Am. Chem. Soc.* **2001**, *123*, 9198−9199.
(16) Park, J. I.; Cheon, J. *J. Am. Chem. Soc.* **2001**, *123*, 5743−5746.
(17) Lu, L.; Wang, H.; Xi, S.; Zhang, H. *J. Mater. Chem.* **2002**, *12*, 156−158.
(18) Riedel, W. *Electroless Nickel Plating*; Finishing Publications: Metals Park, 1991.
(19) Zhang, Y. H.; Yan, T. T.; Yu, S. Q.; Zhuang, S. Y. *J. Electrochem. Soc.* **1999**, *146*, 1270−1272.
(20) Boontongkong, Y.; Cohen, R. E.; Rubner, M. F. *Chem. Mater.* **2000**, *12*, 1628−1633.
(21) Deng, T.; Arias, F.; Ismagilov, R. F.; Kenis, P. J. A.; Whitesides, G. M. *Anal. Chem.* **2000**, *72*, 645−651.

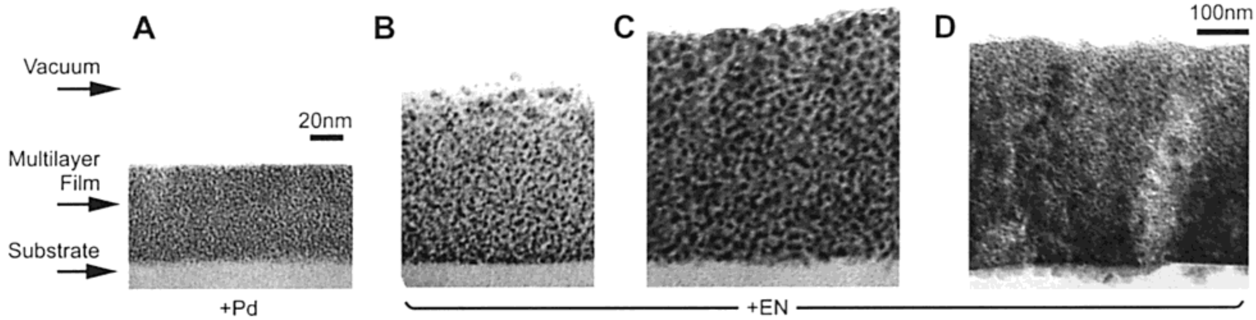

Figure 1. (A) Cross-sectional TEM images of $(PAH3.5/PAA3.5)_{15}(PAH6.5)$ on PS substrates with in situ synthesized Pd nanoparticles, ≈2 nm in diameter (dark contrast). (B, C) Films of (A) after immersion into pH-unadjusted EN solution for 50 min and 19 h. (D) Film of (A) after immersion into EN solution with 0.2 M NH_4OH for 5.3 h. Note the same scale bar applies for (A, B, C) but not (D).

were obtained with minimal underfocus to mitigate any phase contrast structures that may interfere with the accuracy of particle size determination. Features <1 nm could not be reliably distinguished and therefore nanoparticles were not measured at this length scale. Moreover, because of the manual selection of the particles to be measured, the size distributions were biased toward larger, more easily discernible, particles. Energy-dispersive X-ray spectroscopy (EDS) was performed on microtomed cross sections imaged using a JEOL 2010 transmission electron microscope operating at 200 kV with an Oxford Instruments Link Pentafet detector.

Elemental analyses by X-ray photoelectron spectroscopy (XPS) and Auger electron spectroscopy (AES) were performed using a Kratos AXIS Ultra Imaging XPS with an Al Kα source and a Physical Electronics Model 660 Scanning Auger Microscope operating at 5 kV. To minimize charging effects, films for AES were assembled on Si substrates and the sample was wrapped in aluminum foil with a pinhole for the electron probe. XPS was also performed on films supported on Si substrates.

Results

The various films are referred to in shorthand notation, where $(PAHx/PAAy)_z(PAHx')$+Pd indicates a multilayer consisting of z bilayers of PAH and PAA assembled at pH x and y, respectively, with a final adsorbed layer of PAH at pH x' and containing in situ synthesized zerovalent Pd nanoparticles; Pd/Ni refers to nanoparticles that have been further grown by EN deposition. Pd nanoparticles were synthesized within the PAH/PAA multilayers from the reduction of a Pd complex precursor, $[Pd(NH_3)_4]^{2+}$. Small nanoparticles with ≈2-nm diameters, uniformly dispersed throughout the $(PAH3.5/PAA3.5)_{15}(PAH6.5)$ multilayer, were obtained as shown in Figure 1A.

The film containing Pd nanoparticles was immersed into an EN solution with no adjustment of the pH. The nanoparticle size increased with the duration of immersion, as shown in Figure 1B,C. After 50 min, the nanoparticles were ≈3 nm in diameter; after 19 h, they were 4−5 nm. To increase nickel deposition over shorter durations, an EN solution containing 0.2 M NH_4OH was employed (solution pH = 3.7). After only 5 h of immersion into the base-added EN solution, it was difficult to distinguish individual, isolated particles in the multilayer because of considerable nickel deposition, as shown in Figure 1D. EN solutions with even higher base concentrations, such that the pH reached 5 from an original value of 3.3 for example, resulted in gross surface plating of the film in <30 min of immersion.

An estimate of the nickel volume fraction was obtained by comparing the dry thickness of the film before and after immersion into EN solution and by assuming the multilayer itself did not undergo any density changes. The thickness of $(PAH3.5/PAA3.5)_{15}$-$(PAH6.5)$+Pd estimated from the TEM image was ≈59 nm (Figure 1A). The film thicknesses obtained from Figure 1B−D were 100, 137, and 400 nm, corresponding to a nickel content of 41, 57, and 85 vol %, respectively. The calculated volume fractions are consistent with the increased particle diameters.

In $(PAH3.5/PAA3.5)_{15}(PAH6.5)$ multilayers, a relatively high concentration of Pd nanoparticles was formed such that subsequent particle growth by EN deposition quickly made the observation of individual particles, and hence the accurate monitoring of particle size, difficult, as shown in Figure 1D. To reduce the concentration of the Pd nanoparticle population and generate a sparse distribution of seeds, multilayers based on PAH7.5/PAA3.5 were used for in situ Pd nanoparticle synthesis. The concentration of free carboxylic acid groups within this multilayer structure is low,[22] resulting in a low concentration of bound cationic Pd complexes. Figure 2A shows the 60-nm-thick multilayer of $(PAH7.5/PAA3.5)_5(PAH7.5)$ with ≈2-nm-diameter Pd nanoparticles. The relative sparseness of the nanoparticles is not obvious from the cross-sectional TEM image because the image is projected through a 50-nm-thick microtomed slice. After immersion of the Pd nanoparticle-containing multilayer in an EN solution with 0.2 M NH_4OH for 16.5 h, ≈9-nm-diameter particles were obtained, as seen in Figure 2B. In these multilayers, individual nanoparticles could clearly be distinguished, in contrast to the $(PAH3.5/PAA3.5)_{15}(PAH6.5)$ case under the same EN solution conditions. The film thickness had increased to 269 nm, corresponding to 78 vol % nickel. In Figure 2C, a $(PAH7.5/PAA3.5)_5(PAH7.5)$ multilayer with bound cationic Pd complexes, unreduced to zerovalent nanoparticles prior to immersion into the EN solution, shows a dense filling of nickel after electroless deposition. In this case, individual nanoparticles are not distinguishable.

When the same EN solution conditions were applied to a thicker $(PAH7.5/PAA3.5)_{15}(PAH7.5)$+Pd multilayer, a gradient in nanoparticle sizes was obtained, as shown in Figure 3. Larger, ≈14-nm diameter, particles could be seen near the free surface and smaller, ≈3-nm diameter, particles near the substrate. The original

(22) Mendelsohn, J. D.; Barrett, C. J.; Chan, V. V.; Pal, A. J.; Mayes, A. M.; Rubner, M. F. *Langmuir* **2000**, *16*, 5017−5023.

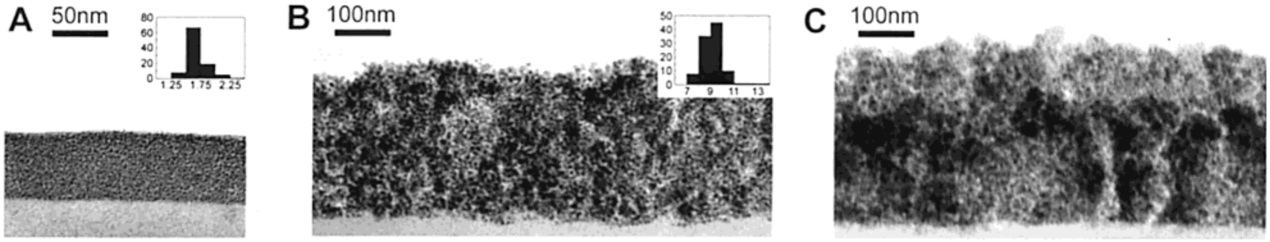

Figure 2. (A) Cross-sectional TEM image of (PAH7.5/PAA3.5)$_5$(PAH7.5) with in situ synthesized Pd nanoparticles (diameter = 1.7 ± 0.2 nm) on a PS substrate. (B) Film of (A) after immersion in EN solution with 0.2 M NH_4OH for 16.5 h (particle diameter = 9 ± 1 nm). (C) (PAH7.5/PAA3.5)$_5$(PAH7.5) with bound $[Pd(NH_3)_4]^{2+}$ after immersion into the same EN solution as (B) for the same duration. Particle diameter histograms in inset; abscissa is diameter (nm) and ordinate is counts.

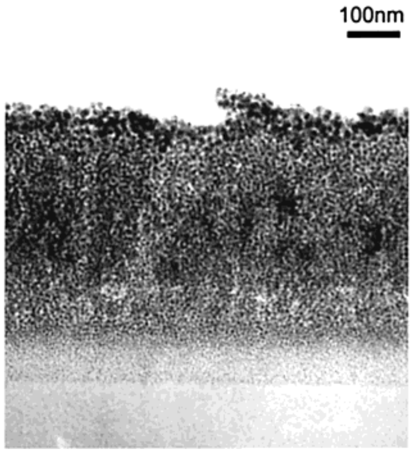

Figure 3. Cross-sectional TEM image of (PAH7.5/PAA3.5)$_{15}$-(PAH7.5) with in situ synthesized Pd nanoparticles after immersion into EN solution with 0.2 M NH_4OH for 15.7 h.

(PAH7.5/PAA3.5)$_{15}$(PAH7.5)+Pd was 150-nm-thick and became 550-nm-thick after nickel deposition, corresponding to 73 vol % nickel.

As a control, a (PAH7.5/PAA3.5)$_5$(PAH7.5)+Pd film was immersed into a solution containing all components of the EN solution except the reductant DMAB for 24 h. No change in Pd nanoparticle size was observed, remaining ≈2 nm in diameter. In addition, a multilayer without Pd was immersed into the EN solution for 24 h; no nickel deposition was observed. Therefore, particle growth in the presence of Pd seeds after immersion into the EN solution resulted from nickel deposition on the seeds, not as a result of seed aggregation.

The Pd seed-mediated growth could also enlarge nanoparticles within heterostructure films composed of PAH/PAA multilayer strata and PAH/PSS multilayer strata. The cationic Pd complex binds selectively to PAH/PAA regions within the heterostructure with subsequent confinement of the Pd nanoparticles in the same regions, as shown in Figure 4A. The heterostructure consisted of (PAH/PAA)$_{10}$(PAH/PSS)$_{30}$(PAH/PAA)$_{10}$-(PAH/PSS)$_{35}$(PAH) assembled at pH 3.5. After immersion in the EN solution without added base for 22.5 h, as shown in Figure 4B, the nanoparticles increased from 2 to 4 nm in diameter, comparable to those in the PAH/PAA-only multilayers. However, with the concomitant increase in thickness of the PAH/PAA strata, the integrity of the PAH/PSS strata appeared to be compromised by the nanoparticles. Because of the salt concentration in the EN solution, ≈0.3 M, the entire multilayer structure was likely swollen.[23] The PAH/PSS stratum next to the free surface was relatively free of

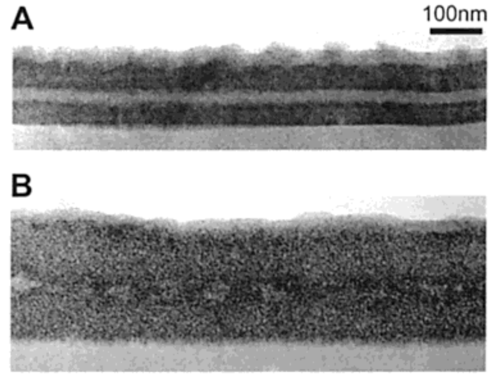

Figure 4. Cross-sectional TEM images of heterostructure (PAH/PAA)$_{10}$(PAH/PSS)$_{30}$(PAH/PAA)$_{10}$(PAH/PSS)$_{35}$(PAH) assembled at pH 3.5 with in situ synthesized Pd nanoparticles (A) before and (B) after immersion into pH-unadjusted EN solution for 22.5 h.

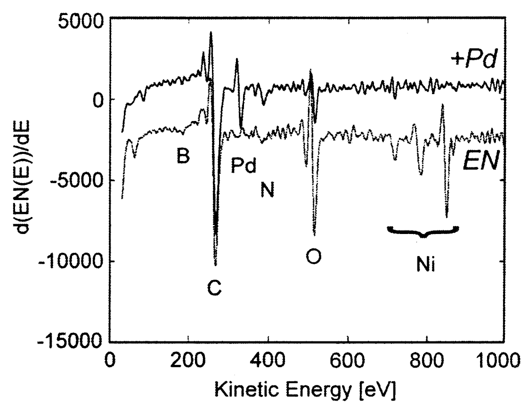

Figure 5. AES elemental survey spectrum of (PAH7.5/PAA3.5)$_5$(PAH7.5)+Pd before (solid trace) and after (dotted trace, offset for clarity) EN deposition. Main Auger lines are labeled.

nanoparticles compared to the PAH/PSS stratum sandwiched between the two PAH/PAA strata.

AES and XPS were employed to probe the composition of the nanoparticles, at least those near the multilayer surface, after EN deposition. Figure 5 shows the elemental survey from AES of (PAH7.5/PAA3.5)$_5$-(PAH7.5)+Pd and (PAH7.5/PAA3.5)$_5$(PAH7.5)+Pd/Ni.[24] Their corresponding cross-sectional TEM images are Figure 2A,B. From the Auger spectrum of the +Pd film, Pd was identified along with the other elements that

(23) Dubas, S. T.; Schlenoff, J. B. *Langmuir* **2001**, *17*, 7725−7727.

(24) The elemental composition within the +Pd/Ni film was also confirmed by EDS analysis on a TEM cross-sectioned sample (Figure 2B) and indicated the presence of Ni and Pd as expected; B was too light for the detector.

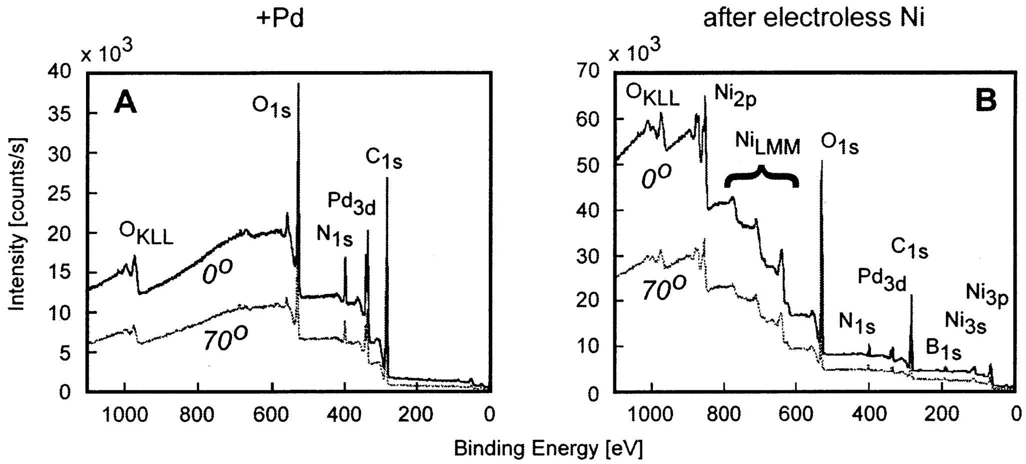

Figure 6. XPS elemental survey spectra of $(PAH7.5/PAA3.5)_5(PAH7.5)$+Pd (A) before and (B) after EN deposition at normal (0°, solid traces) and grazing (70° from normal, dotted traces) angles of detection relative to the surface plane.

Table 1. Quantitative Elemental Analysis by XPS

element	Pd(0) sample normal angle	Pd(0) sample grazing angle	after EN normal angle	after EN grazing angle
B:Ni (atomic ratio)			0.32	0.23
B:Ni (mass ratio)			0.059	0.042
Pd:N (atomic ratio)[a]	0.34	0.34	0.036	0.034
Ni:N (atomic ratio)[a]			0.92	0.84
B:N (atomic ratio)[a]			0.30	0.19

[a] For sample after EN, atomic ratios relative to N multiplied by 0.22 for polymer volume fraction.

comprise the polyelectrolytes of the multilayer—C, N, and O. In the +Pd/Ni Auger spectrum, the Ni signal was clearly observed and the Pd signal was diminished to within the background noise. In addition, a small B signal was detected and the O signal was larger than in the +Pd spectrum. Boron from DMAB is known to be incorporated[25] into the deposited Ni. The increased O likely corresponds to the Ni native oxide.

XPS analysis was performed on the same AES samples to obtain quantitative elemental compositions as well as nondestructive, depth profile information. Figure 6A shows the XPS spectra for $(PAH7.5/PAA3.5)_5$-(PAH7.5)+Pd with the detector at normal (0°) and grazing (70°) angles. As with the AES analysis, Pd was detected along with the elements comprising PAH and PAA. The XPS spectra for $(PAH7.5/PAA3.5)_5$-(PAH7.5)+Pd/Ni, in Figure 6B, additionally show the characteristic photoelectrons for Ni and B.

The quantitative elemental analysis from XPS is reported in Table 1. The boron content in the electroless nickel was consistent with compositions reported of electrolessly plated nickel from aminoborane-based solutions.[26] For comparison of +Pd and +Pd/Ni samples, the elements of interest were scaled relative to the N signal, which should only come from the PAH ammonium groups in the film, and the volume fraction of polymer.[27] Because the escape depth of primary Pd Auger and photoelectrons is on the order of 1 nm through an inorganic solid,[28] and with the Pd/Ni nanoparticle having 9-nm diameter, a Ni shell of ≈3.5 nm around a 2-nm-diameter Pd core should attenuate a good number of the electrons. The diminishment of Pd Auger and photoelectrons from the +Pd/Ni spectrum is consistent with a core—shell structure, as expected from the electroless metal chemistry. Although this evidence is not conclusive, electroless silver[14] and electroless copper[19] depositions have been shown to overcoat gold colloids. Finally, the comparable compositions obtained at different detection angles for the +Pd and +Pd/Ni samples indicate that the compositions reflect the nanoparticles and not an anomalous surface monolayer.

Discussion

Two important considerations distinguish the use of seed-mediated growth to control nanoparticle size within polyelectrolyte multilayers from the use of this approach in solution: a heterogeneous reaction environment with various different interfaces and significant mass-transport limitations. First, one must consider the reaction environment at the surface of the multilayer as well as the one inside the multilayer. The surfaces of PAH/PAA multilayers assembled at a low pH are rich in carboxylic acid groups,[29] which can bind the cationic Pd complex and form large surface nanoparticles. Our objective was to target the electroless deposition of nickel on the Pd seed particles inside the film and not on the film surface. The surface should ideally be free of Pd particles. If the surface activity were not capped or quenched, nickel would plate on the surface and eventually hinder any diffusion of reactants into the multilayer interior to the detriment of further particle growth. Therefore, for the PAH3.5/PAA3.5 multilayers, the last layer of PAH was adsorbed at higher pH to

(27) To account for the difference in the amount of polymer, and hence N, probed by XPS between +Pd and +Pd/Ni samples, the reported element ratios for the +Pd/Ni sample were multiplied by the volume fraction of polymer, 0.22, approximated by the ratio of the thicknesses of the two samples.

(25) Lelental, M. *J. Electrochem. Soc.* **1973**, *120*, 1650–1654.
(26) Safranek, W. H. *The Properties of Electrodeposited Metals and Alloys*, 2nd ed.; American Electroplaters and Surface Finishers Society: Orlando, 1986.
(28) Ferguson, I. F. *Auger Microprobe Analysis*; Adam Hilger: Bristol, 1989.
(29) Yoo, D.; Shiratori, S. S.; Rubner, M. F. *Macromolecules* **1998**, *31*, 4309–4318.

obtain a much thicker PAH outermost layer that buried the PAA underneath.[30] For PAH7.5/PAA3.5 multilayers, the PAH last layer sufficiently prevents any Pd complex binding at the surface.[31]

Second, the balance between reaction rate and mass-transfer rate of the reactants is crucial in obtaining uniform seed-mediated particle growth throughout the film. In solution, the electroless metal deposition rate is reaction-limited. However, because of the lower diffusivity within the multilayers relative to that in solution, mass-transfer-limited metal deposition can readily occur as seen in Figure 3. At the extreme when the reaction rate is instantaneous relative to mass transfer, pure surface plating occurs. While a relatively slow mass transfer can be used to create a gradient of nanoparticle sizes, to obtain nanoparticles of the same size throughout the film, the reaction rate must be made limiting relative to the mass-transport rate within the multilayer. Important kinetic parameters of the electroless chemistry include the reductant concentration, pH, and temperature.[18] The pH of the EN solution could be manipulated easily without affecting the mass transfer of the nickel precursor and reductant. When the EN solution was kept more acidic (i.e., not raising the pH by adding NH_4OH, as is normally done for EN plating on surfaces), the reaction was sufficiently slow such that the reactants could access the film interior.

Ideally, EN deposition should continue to grow individual nanoparticles until they coalesce. With low initial seed concentrations, a wide size range should be accessible before the particles touch while with high initial seed concentrations, the growing particles would quickly grow into one another. However, even for the films with nickel in excess of 70 vol %, percolation of the particles was not observed by in-plane resistivity measurements. In addition, EN deposition durations longer than 24 h did not continue to grow larger particles. These observations could be rationalized by the increased hindrance to reactant diffusion into the multilayer film as more nickel is deposited, thereby self-limiting the growth of individual particles before any substantial coalescence or percolation. The polymeric matrix may also interfere with particle coalescence. Moreover, after long deposition times, the accumulation of byproducts, which results in pH depression, and the depletion of the reductant by a competing hydrolysis reaction contribute to particle growth suppression; the EN solution could be recharged by replenishment.

Nevertheless, particles of controlled size with a magnetic shell around a polarizable core could be grown successfully by electroless chemistry within the multilayers. These thin film nanocomposites should show interesting magnetic properties and have potential magnetic media applications,[16,32−34] which we are currently investigating.

Conclusions

The growth of nickel onto in situ synthesized Pd nanoparticles within PAH/PAA multilayers was facilitated by EN deposition. By controlling the nickel deposition rate via solution pH and the duration of deposition, 2-nm-diameter Pd nanoparticles could be overcoated with a nickel shell, resulting in particles up to 14 nm in diameter. Not only was the EN deposition a faster route to larger nanoparticles than our previous ion exchange and reaction approach, nanoparticle size could be controlled independently of nanoparticle concentration.

Acknowledgment. We thank Elisabeth L. Shaw of the MIT Center for Materials Science and Engineering (CMSE) for assistance with AES and XPS. This work was supported by the MIT MRSEC Program of the National Science Foundation under award number DMR 94-00334 and made use of shared experimental facilities at the MIT CMSE.

CM020934H

(30) Shiratori, S. S.; Rubner, M. F. *Macromolecules* **2000**, *33*, 4213−4219.
(31) Wang, T. C.; Chen, B.; Rubner, M. F.; Cohen, R. E. *Langmuir* **2001**, *17*, 6610−6615.
(32) Ziolo, R. F.; Giannelis, E. P.; Weinstein, B. A.; O'Horo, M. P.; Ganguly, B. N.; Mehrotra, V.; Russell, M. W.; Huffman, D. R. *Science* **1992**, *257*, 219−223.
(33) Sohn, B. H.; Cohen, R. E.; Papaefthymiou, G. C. *J. Magn. Magn. Mater.* **1998**, *182*, 216−224.
(34) Sun, S.; Anders, S.; Hamann, H. F.; Thiele, J.; Baglin, J. E. E.; Thomson, T.; Fullerton, E. E.; Murray, C. B.; Terris, B. D. *J. Am. Chem. Soc.* **2002**, *124*, 2884−2885.